An Open-Source Plate Reader

Karol P. Szymula, Michael S. Magaraci, Michael Patterson, Andrew Clark, Sevile G. Mannickarottu, and Brian Y. Chow*

Department of Bioengineering, University of Pennsylvania, 210 South 33rd Street, Philadelphia, Pennsylvania 19104, United States

Supporting Information

Downloaded via UNIV OF PENNSYLVANIA on March 7, 2019 at 23:04:49 (UTC). See https://pubs.acs.org/sharingguidelines for options on how to legitimately share published articles.



ABSTRACT: Microplate readers are foundational instruments in experimental biology and bioengineering that enable multiplexed spectrophotometric measurements. To enhance their accessibility, we here report the design, construction, validation, and benchmarking of an open-source microplate reader. The system features full-spectrum absorbance and fluorescence emission detection, in situ optogenetic stimulation, and stand-alone touch screen programming of automated assay protocols. The total system costs less than \$3500, a fraction of the cost of commercial plate readers, and can detect the fluorescence of common dyes at concentrations as low as ~10 nM. Functional capabilities were demonstrated in the context of synthetic biology, optogenetics, and photosensory biology: by steady-state measurements of ligand-induced reporter gene expression in a model of bacterial quorum sensing and by flavin photocycling kinetic measurements of a LOV (light-oxygenvoltage) domain photoreceptor used for optogenetic transcriptional activation. Fully detailed guides for assembling the device and automating it using the custom Python-based API (Application Program Interface) are provided. This work contributes a key technology to the growing community-wide infrastructure of open-source biology-focused hardware, whose creation is facilitated by rapid prototyping capabilities and low-cost electronics, optoelectronics, and microcomputers.

he creation of open-source hardware for enabling molecular and cellular studies is facilitated by the ready availability of rapid prototyping techniques, low-cost optoelectronics, and commoditized microcomputers and microcontrollers. Such open-source platforms—which to date include fluorescence imagers, ^{1,2} spectrophotometers, ³ turbidostats, ⁴ robotic liquid handlers, ^{5,6} and multiwell plate illuminators for optogenetic stimulation 7,8—increase access to both standard and custom laboratory apparatus alike. Here, we report the creation of an open-source plate reader (OSP), which is one of the most ubiquitous and important technologies in experimental biochemistry, biology, and bioengineering, because a plate reader permits automated and multiplexed spectrophotometric measurements.

Plate readers typically consist of a multimode (absorbance/ optical density and fluorescence) spectrophotometer and a programmable-motion stage for multiplexing by serial positioning of sample wells of the plate over a single detector. Detection wavelengths are selected using diffraction gratings or dichroic filters, and excitation wavelengths are selected similarly or by using monochromatic or narrow-band excitation sources such as lasers and light-emitting diodes (LEDs). They may possess auxiliary input ports for fluid delivery, and these ports have been successfully co-opted for other purposes such as optogenetic stimulation. However, commercial plate readers cost tens of thousands of U.S. dollars, which can be prohibitive for resource-limited environments, including educational settings.

The open-source framework (Figure 1) reported here is intended to provide the necessary and modular functionalities of a commercial system while maintaining the performance required for most assays at a fractional cost (less than \$3500 or an ~10-fold reduction). The system features full-visiblespectrum absorbance and fluorescence emission capabilities, in situ optogenetic stimulation, and stand-alone touch screen programming of automated assay protocols. It is expandable and customizable, with built-in access and communication ports for external modules to enhance function and its own

Received: September 6, 2018 Revised: November 30, 2018 Published: December 4, 2018

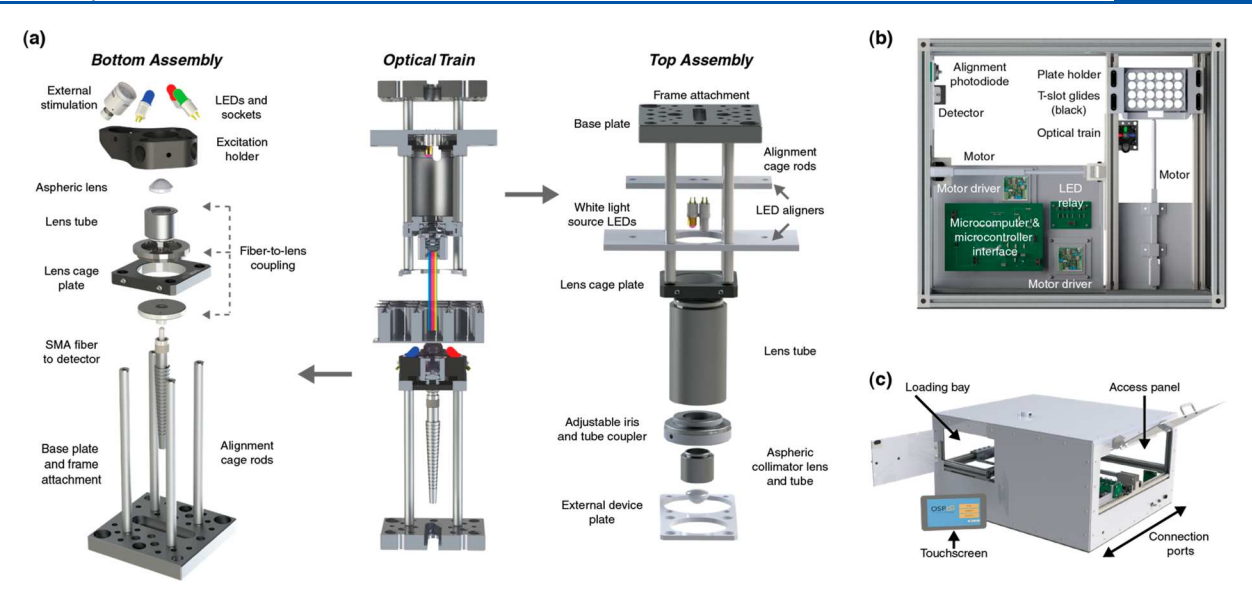


Figure 1. Opto-mechanical summary of the open-source plate reader (OSP). All images are CAD renderings. (a) The optical train, with exploded views of the bottom assembly for detection and optical excitation and the top assembly for the white light source for optical density measurements and for external devices (e.g., high-power optogenetic stimulation or fluid delivery). The white light source combines two LEDs to span the visible spectrum. (b) Top-down view of the whole instrument. The relay board contains header blocks that consolidate connections of the individual device components, separated from the main microcomputer board. The top optical train has been omitted for the sake of clarity. (c) Isometric view of the instrument, with a touchscreen that can be mounted. All connections and access for repair are consolidated on one side.

Python-based Application Programming Interface (API). We document the design considerations, overview of system assembly and operation, benchmarking with standard fluorochrome dyes, and validation in molecular and cellular level experiments in synthetic biology, optogenetics, and photobiology contexts.

RESULTS AND DISCUSSION

Opto-Mechanical Platform Design. The fundamental core of a plate reader is two-axis motion for *x*–*y* positioning with respect to a single set of fiber-optic input/outputs, which enables multiplexing. Thus, we designed low-cost hardware and software frameworks (Figures 1 and 2) for automated motion and for interfacing with open-source devices and fiber-coupled optoelectronics. For baseline functionality that is useful in most laboratory contexts, the OSP employs a CCD (charge-coupled device) linear array detector with open-source

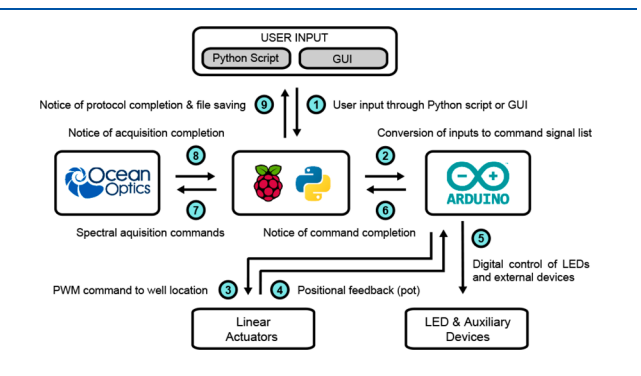


Figure 2. Device integration and automation workflow. User inputs to a Raspberry Pi microcomputer (center) are entered via the graphical user interface (GUI) or written Python script. The microcomputer coordinates the inputs and outputs to all other components. Abbreviations: PWM, pulse width modulation; pot, potentiometer value; LED, light-emitting diode.

drivers (Ocean Optics) and inexpensive dome-capped LEDs as illumination sources for absorbance/optical density (OD) measurements and for fluorescence measurements with common fluorochromes (Figure 1a). The use of fiber optics to couple the optical elements to the sampling location allows for modular choice in excitation sources and detectors and, importantly, also supports the expansion or customization through these optical fibers to more sensitive detectors or to sources of higher power or different wavelengths. Thus, the system is designed as a low-cost and expandable plate reader chassis.

For automated motion, a custom three-dimensionally printed (3D-printed) plate holder is attached to low-cost linear drive motors that provide positional feedback voltage readings. The motors were chosen to ensure a sufficient travel range (140 mm) for plate loading and load-bearing capacity (100 N) for the plate stage. The motor-connected stage glides on a modular frame of extruded t-slotted aluminum, which was chosen for its ease of assembly and the utility of the t-slot tracks themselves for alignment, similar to dovetail rails (Figure 1b). Plates are tightly and repeatably positioned into one corner of the holder by spring-loading and loaded through a front door (Figure 1c).

For optical detection, an optomechanical lens cage assembly under the plate holds a collimating aspheric lens to couple transmitted and emitted (bottom fluorescence) light to a multimode fiber-optic cable (Figure 1a, left). This patch cord can be connected to any fiber-compatible detector with a SMA fitting. In the baseline low-cost version here, we use a CCD-based Ocean Optics visible-range detector because of its available open-source drivers and overall balance of sensitivity, full-spectrum and monochromatic detection, and relatively low cost compared to those of monochromator-coupled photomultiplier tubes (PMTs).

For bottom fluorescence excitation, a 3D-printed component surrounds the detector fiber input assembly and projects multiple light sources onto the plate bottom. Three positions

hold socket connectors for dome-capped LEDs as cost-effective, bright, and built-in fluorescence excitation sources. Initially, these LEDs are blue, green, and orange (λ = 470, 525, and 610 nm, respectively) for exciting common dyes and fluorescent proteins, but they can be simply replaced with different standard dome-capped LEDs. In lieu of using collimating lenses, the LEDs have narrow solid angles that, combined with the acceptance angle of the collection aspheric, prevent well-to-well crosstalk. These LEDs can also be used for optogenetic stimulation. The OSP was designed for visible-spectrum measurements of most plate reader assays and, thus like any commercial filter-based plate reader, omits a fully tunable excitation source like a scanning monochromator for fluorescence excitation scans.

An additional position of the projection assembly holds an SMA-terminated fiber optic collimating lens for use with external sources as alternatives or upgrades to dome-capped LEDs. For cases in which the user requires multiple external sources coupled to the one collimated projection fiber, we suggest commercially available bifurcated or fan-out optical fibers (e.g., from Thorlabs) as a cost-effective alternative to traditional dichroic beam combiners, because the fiber-based solution is effectively universal by eliminating the minimum spectral separation needed for co-aligning optical sources with dichroic mirrors. However, such combiners are not recommended for co-aligning a detection fiber with excitation sources (i.e., 90° incident angle between the sample and excitation), because direct back reflection from a collimating lens or plate bottom saturates the detector in the absence of an automated dichroic filter wheel or tunable diffraction gratings.

For top-side excitation for absorbance/optical density measurements and optogenetic stimulation, another optomechanical lens train (Figure 1a, right) over the plate positions a visible-spectrum white light source, consisting of two LEDs (LED1, $\lambda = 430-660 \text{ nm}$; LED2, $\lambda = 430 \text{ nm}$) (Figure S1). A laser-cut component connected to the top optical train positions an auxiliary port for external functionality like fluid delivery and optogenetic stimulation. Similar to commercial systems, the auxiliary port is spatially offset from the detector with an ~5 s delay between the delivery of fluid/photons to the well and measurement from the well, although simultaneous zero-delay optogenetic stimulation is possible using the bottom excitation sources. The auxiliary port is designed to couple to a standard optical lens cage plate for attaching and aligning custom components, which can be fed into the OSP through a grommet on top.

Automation and Interface Design. The OSP can be operated by an external computer or Raspberry Pi microcomputer by using automated scripts or a graphical user interface (GUI) that supports touchscreen control (Figure 2). The GUI and automation software are programmed in Python. The description of the interface will assume the use of a Raspberry Pi hereafter for the sake of simplicity.

The Raspberry Pi/computer communicates directly with the detector to set acquisition parameters and also sends programming commands to an Arduino microcontroller (Figure S2 and Supporting Note 1). The Arduino controls the other functions (LEDs, motors, and auxiliary functions) and synchronizes them with the detector data acquisition through digital logic. The LED timing is controlled by digital switching of a transistor-gated current source. The motors are controlled by pulse width modulation commands sent to the commercial motor driver-boards, which also relay positional

feedback (potentiometer readings). Auxiliary functions can be triggered by standard digital logic control of external devices. The Arduino serves as the input/output hub because the Raspberry Pi lacks general purpose analog inputs for positional feedback from the motors and alignment photodiode, without the use of an analog-to-digital converter (ADC). Furthermore, the instrument control architecture is preserved if another type of computer is substituted for the Raspberry Pi microcomputer.

The GUI (Supporting Note 1) emulates the basic programming capabilities of commercial plate readers. Acquisition parameters include (i) the detector integration time, (ii) the selected data range for spectra (scan averaging, excitation wavelength), (iii) the time step for kinetic acquisition, (iv) well selection and control [ordering, calibration (Figure S3), and shaking], and (v) coordination with auxiliary functions. Data spreadsheets are exported to local storage and can be manipulated locally in the Raspberry Pi environment using the open-source office software suite, LibreOffice (or a similar suite).

Protocols: Device Construction and Operation. Detailed step-by-step assembly guides and a programming overview are available (Supporting Notes 1-4), as summarized here. Supporting Note 1 describes software installation, the organization of the open-source API, the available functions for custom programming, and a walk-through of the GUI operation. Supporting Note 2 provides assembly instructions for the top and bottom optical trains shown in Figure 1a. Supporting Note 3 describes the assembly of the printed circuit boards and the photodiode assembly used for calibrating the spatial coordinates of the motor. Supporting Note 4 provides overall assembly instructions of the t-slotted frame, all custom 3D-printed or laser-cut components, including the plate stage (Supporting File 1), and the integration of all subcomponents (trains, circuit boards, stage, and frame), into a complete device. The total cost of the system is less than \$3500 (Table

The use of lens cage assemblies allows for facile alignment of all optical components along the detection axis (Supporting Note 3). To initialize the spatial coordinates of the microplate wells postassembly (Figure S3), transmission measurements are made through a mask overlaid on the plate, as detected by a fast photodiode (Figure 1b); an automated script identifies the center of three alignment wells and the plate edges to define the spatial map. This calibration protocol takes ~3 min, which is short enough to regularly perform to ensure repeatability.

A disk image file for software installation (OSP.img) is available via a permanent link at the University of Pennsylvania's Scholarly Commons, where all necessary guides, schematics, software, and CAD files will be updated with version improvements; the content of this site is mirrored at the GitHub software repository. CAD files and assembly guides are also available on the MetaFluidics CAD repository. The links can be found in Associated Content.

The 3D-printed parts were made from PLA (polylactic acid) filament, the most common material for desktop 3D-printers. Most 3D-printable polymers would be suitable unless they were water-soluble in the event a spill {e.g., PVA [poly(vinyl alcohol)]} or they were soft [e.g., low-density polyethylene (LDPE)] or flexible (e.g., rubberized "flexible filament") materials that hold poorly over time when fastened under compression. Alternatively, the plate holder can be milled from

metals and machinable rigid plastics like Delrin (polyoxymethylene). Laser-cut parts were made from an acrylic sheet, which is suitably stiff for fastening under compression and for remaining flat as a supported wall/floor (as is Delrin). Alternatively, the two-dimensional components can be machined from other hard sheets like metal, Lexan (polycarbonate), or PVC (polyvinyl chloride), although these materials are incompatible with a $\rm CO_2$ laser cutter. Woodbased materials are unsuitable for any component that requires dimensional stability because they swell with moisture.

Performance Benchmarking with Reference Dyes. The baseline system performance was assessed using a reference standard fluorescent dye kit (Figure 3). The

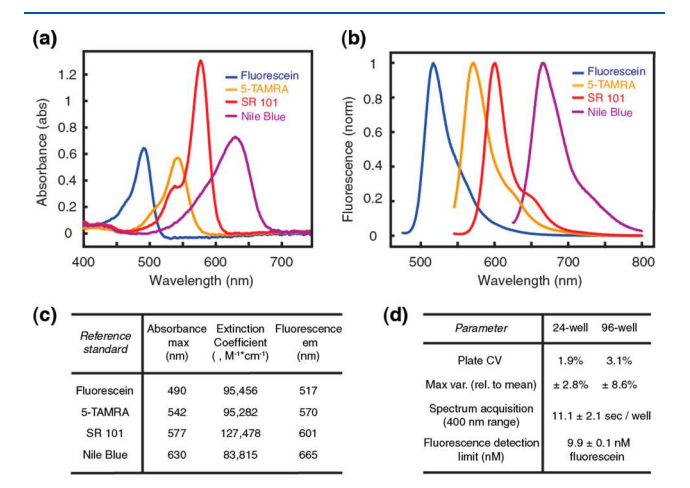


Figure 3. Characterization of the OSP using reference dyes. Measurements were made according to commercial protocols (Thermo R14872). Abbreviations: 5-TAMRA, 5-carboxytetramethylrhodamine; SR 101, sulforhodamine 101. (a) Absorbance spectra. (b) Fluorescence emission spectrum. (c) Key measured spectral parameters from panels a and b. (d) Key performance ranges. Abbreviations: CV, coefficient of variation across the plate; Max var., variation range across the plate. The spectrum acquisition time with a 1.25 s integration and stage motion to the well. The detection limit error is the standard deviation.

respective absorbance/emission peak spectra and extinction coefficients of the dyes were in line with expected values. Thus, the custom opto-mechanical elements do not introduce major aberrations. The fluorescence of NIST-traceable fluorescein could be measured with an $\sim \! 10$ nM limit of detection with the low-cost detector. Such a detection limit is sufficient for common fluorescence assays as intended, albeit greater than the $\sim \! 10$ pM limit of commercial systems that use PMTs.

The spectral separation required between the fluorescence excitation and emission detection starting wavelengths was approximately one fwhm (full width at half-maximum) of an LED because of the collection of reflected light from the plate bottom (Figure S4). Given a typical ~30 nm fwhm of domecapped LEDs here, the separation is on par with the recommended separation of a commercial plate reader. The separation can be decreased as low-cost LEDs with narrower bandwidths become available, or with laser diodes.

The coefficients of variation across entire 24-well or 96-well plates were 1.9 and 3.1%, respectively, with maximum variations from the mean of 2.8 and 8.6%, respectively. The variability is largely set by the motor resolution (vs that of high-precision stepper motors that are ~50-fold more expensive). The precision is sufficient for these common 24-

well and 96-well plate formats, albeit unlikely for higher-density 384-well plates and beyond.

The OSP acquires a full spectrum in ~ 11 s per well (inclusive of the movement to the well). Because the CCD detector captures all wavelengths simultaneously, the acquisition time for a full spectrum is the same as that of a single wavelength measurement. While a commercial plate reader with a PMT detects single wavelengths in roughly the same amount of time, the latter is much slower when measuring full spectra because it sweeps individual wavelengths; as a matter of reference, in our hands a Tecan microplate reader takes nearly 6 min to acquire a spectrum (400 nm-wide range with 2 nm step size). This difference in time can be meaningful with samples in organic solvents prone to evaporation or samples prone to sedimentation.

Validation in Cellular and Biomolecular Contexts. We performed cellular and protein level assays to demonstrate the standard and nonstandard measurement functionalities of the OSP in biomolecular contexts. First, we measured the input/output transfer functions of bacterial "Receiver" strains, ^{1,10} in which fluorescent protein reporter expression is placed under the switchlike transcriptional regulation of the (acyl-homoserine-lactone) AHL-responsive *luxR* activator (Figure 4). This

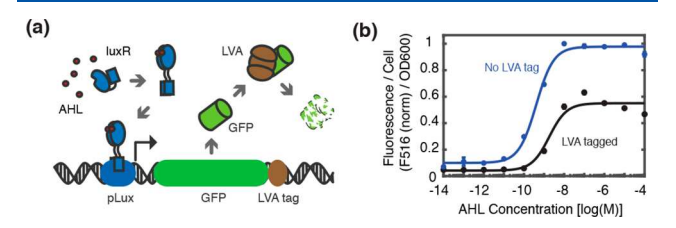


Figure 4. Cellular assays of a model of bacterial quorum sensing. (a) Schematized genetic circuit of GFP expressed under the transcriptional regulation of the AHL ligand-inducible luxR transcriptional activator and under the post-translational degradatory regulation of LVA protease. (b) Transfer function between the AHL input and GFP fluorescence output, with and without the LVA tag. Switching point values agree with those of previous reports F516 is the fluorescence at $\lambda = 516$ nm, scaled to the maximum. OD600 is the optical density at $\lambda = 600$ nm. The error is the standard error of the mean (N=3).

system was chosen for its widespread use in synthetic biology to systematically study transcriptional regulation and intercellular communication ^{10,11} and also because it involves the two major functionalities of a plate reader of transmission measurements (optical density) and fluorescence measurements needed to determine OD-normalized cellular fluorescence. The two *Escherichia coli* strains differ by the presence or absence of an LVA degradation tag^{12,13} on the GFP reporter. The relative switching behaviors of these strains are consistent with our previously reported measurements on a commercial (Tecan) plate reader (see BC-A1-001 and BC-A1-002 in the Supplement of ref 1) with respect to the half-saturation concentration of AHL and the relative magnitudes of GFP expression.

Next, we measured the flavin photocycling ¹⁴ kinetics of light-oxygen-voltage (LOV) domain photoreceptor EL222 from purified recombinant protein (Figure 5). ¹⁵ This kinetic measurement (absorbance at 450 nm, A_{450}) monitors the blue light-induced formation and thermal reversion (in the dark) of a cysteinyl-flavin photoadduct that underlies photosensory signaling by LOV proteins, which are of great importance in

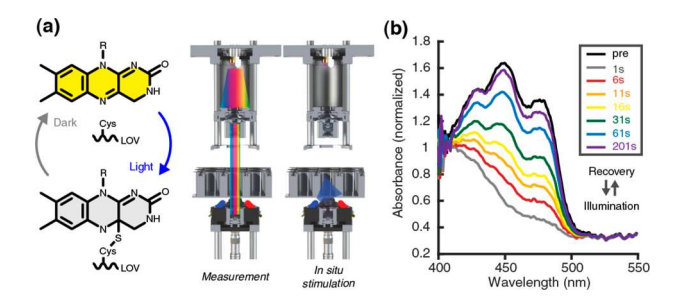


Figure 5. Flavin photocycling of EL222 by *in situ* optogenetic stimulation. (a) Flavin photoadduct formation and/or reversion in a LOV sensor domain, measured by absorbance spectroscopy with *in situ* stimulation (λ = 470 nm at 10 mW/cm², 5 s). (b) Representative flavin photocycling of 37 μ M FPLC-purified recombinant holoprotein, normalized to its isosbestic point. The triplet peak vibronic structure could be resolved, and the measured thermal reversion kinetics (τ = 31.5 s, confidence interval of \pm 0.5 s, N = 3; 5 s sampling interval, measured at λ = 450 nm) were in agreement with reported values. Pre indicates preoptogenetic stimulation, taken in the dark. Times are post-illumination recoveries in the dark.

photobiology and pervasive in optogenetics and synthetic biology. ^{16,17} EL222 in particular is commonly studied to explore the protein structure-function relationships of light-induced homodimerization, and the bacterial LOV is useful for light-activated transcriptional activation with high on/off contrast ratios in eukaryotes. ^{18,19} The photocycling measurement demonstrates the ability to measure a kinetic time course and coordinate the measurement with a programmed set of events, in this case, *in situ* optogenetic stimulation of an individual well. To date, such *in situ* illumination for multiplexed measurements requires custom modification of a commercial plate reader. ⁹

In summary, we report the design, construction, and validation of an open-source plate reader framework. The cost effectiveness of the OSP highlights the importance to laboratory research of rapid prototyping technologies, low-cost solid-state optoelectronics, and minimal single-board microcomputers and microcontrollers. The open-source nature and modularity of the system will facilitate future customization or enhancements that incorporate improved components as they decrease in cost, such as high-power collimated LEDs and the use of metal 3D-printing. The low-cost, modular, and expandable plate reader will enhance access to, and flexibility of, a core instrument across biological and chemical disciplines.

MATERIALS AND METHODS

The parts list (including raw materials and vendors), step-bystep guides for hardware construction and calibration, and software installation and application programming can be found in the Supporting Information, as described in Protocols: Device Construction and Operation.

Circuit boards were printed by Advanced Circuits. T-Slotted aluminum was cut to specification by 8020, Inc. Custom mechanical components were designed in Solidworks and fabricated at the George H. Stephenson Bioengineering Education Laboratory at the University of Pennsylvania. Laser-cut parts were made on a Universal Laser Systems VLS 3.50 with acrylic sheets. 3D-printed parts were made on a MakerBot Replicator (5th Generation) with polylactic acid (PLA) filament. Custom mechanical components can be produced at a facility with similar equipment for rapid

prototyping or CNC machining (mill and waterjet cutting), such as a local/university machine shop or commercial service (e.g., eMachineShop).

All assays were cross-validated on a commercial Tecan Infinite M200 plate reader. The volume-dependent effective path length in 24-well plates was calculated from Beer's law plots of NIST-traceable fluorescein (F36915, NIST Standard Reference Material 1932²⁰) at A_{490} assuming $\varepsilon = 87000 \text{ M}^{-1}$ cm^{-1} (conversion factor of 2.18 mL of fluid for an \sim 1 cm effective path length, linear down to a volume of 500 μ L). Reference dye measurements were performed according to the kit manufacturer's protocols (Thermo Fisher R14782), using an integration period of 1.25 s. Quorum sensing experiments were performed as described previously. Recombinant EL222 was bacterially produced and FPLC-purified as described previously. 21 The fluorescence detection limit was measured by reported methods for determining plate reader sensitivity, 22 with 0.3 μM NIST-traceable fluorescein and an integration time of 1.25 s.

Associated Content. Repository. Penn Scholarly Commons: https://repository.upenn.edu/be_papers/221/. GitHub: https://github.com/brianchowlab/OSP. MetaFluidics: https://metafluidics.org/devices/open-source-plate-reader/.

ASSOCIATED CONTENT

S Supporting Information

The Supporting Information is available free of charge on the ACS Publications website at DOI: 10.1021/acs.biochem.8b00952.

Zip file containing CAD files for all custom components and adapters. Future updates will be posted at the University of Pennsylvania Scholarly Commons, through a permanent link. The site content is mirrored at the GitHub and MetaFluidics repositories (ZIP)

Parts list (including raw materials and vendors) and cost summary (Table S1) (PDF)

Software guide (PDF)

Optical train subcomponent assembly guide (PDF)

PCB and photodiode subcomponent assembly guide (PDF)

General assembly guide (PDF)

White light-source spectrum (Figure S1), API workflow (Figure S2), calibration of plate spatial coordinates (Figure S3), and fluorescence spectra without long-pass removal of excitation (Figure S4) (PDF)

AUTHOR INFORMATION

Corresponding Author

*Address: 210 S. 33rd St., Skirkanich Hall Suite 240, Philadelphia, PA 19104. E-mail: bchow@seas.upenn.edu. Phone: (215) 898-5159.

ORCID ®

Karol P. Szymula: 0000-0003-1822-0688 Michael S. Magaraci: 0000-0001-6800-0101 Brian Y. Chow: 0000-0001-6784-6404

Author Contributions

K.P.S. and M.S.M contributed equally to this work and conducted all experiments. K.P.S., M.S.M., and M.P. constructed the device and application programming environment. A.C. contributed to device development. S.G.M. and B.Y.C. coordinated efforts. K.P.S., M.S.M., and B.Y.C. analyzed

data and prepared the manuscript and assembly guides. K.P.S., M.P., and A.C. conducted their work as Penn iGEM 2017.

Funding

This work was funded by the George H. Stephenson Foundation, the University of Pennsylvania Department of Bioengineering, the University of Pennsylvania Office of Vice Provost for Research (VPR), the National Science Foundation (NSF, CAREER Award MCB 652003), and the National Institutes of Health (NIH, R01NS101106). M.S.M. was partially supported by an NSF GRFP Award.

Notes

The authors declare no competing financial interest.

ACKNOWLEDGMENTS

The authors thank Chris Fang-Yen for helpful discussion about optical train design, Thomas Gilgenast for helpful discussion about API design, Erin Berlew for EL222 recombinant protein production, and Kevin Gardner for the EL222 plasmid. The Ocean Optic logo was used with permission from the company; the OSP is not a product of the company. The OSP development was not sponsored by any component manufacturer or commercial service described herein.

REFERENCES

- (1) Magaraci, M. S., Bermudez, J. G., Yogish, D., Pak, D. H., Mollov, V., Tycko, J., Issadore, D., Mannickarottu, S. G., and Chow, B. Y. (2016) Toolbox for Exploring Modular Gene Regulation in Synthetic Biology Training. *ACS Synth. Biol.* 5, 781–785.
- (2) Nuñez, I., Matute, T., Herrera, R., Keymer, J., Marzullo, T., Rudge, T., and Federici, F. (2017) Low cost and open source multifluorescence imaging system for teaching and research in biology and bioengineering. *PLoS One 12*, e0187163.
- (3) Albert, D. R., Todt, M. A., and Davis, H. F. (2012) A Low-Cost Quantitative Absorption Spectrophotometer. *J. Chem. Educ.* 89, 1432–1435.
- (4) Takahashi, C. N., Miller, A. W., Ekness, F., Dunham, M. J., and Klavins, E. (2015) A Low Cost, Customizable Turbidostat for Use in Synthetic Circuit Characterization. *ACS Synth. Biol.* 4, 32–38.
- (5) Gerber, L. C., Calasanz-Kaiser, A., Hyman, L., Voitiuk, K., Patil, U., and Riedel-Kruse, I. H. (2017) Liquid-handling Lego robots and experiments for STEM education and research. *PLoS Biol.* 15, e2001413.
- (6) Steffens, S., Nüßer, L., Seiler, T.-B., Ruchter, N., Schumann, M., Döring, R., Cofalla, C., Ostfeld, A., Salomons, E., Schüttrumpf, H., Hollert, H., and Brinkmann, M. (2017) A versatile and low-cost open source pipetting robot for automation of toxicological and ecotoxicological bioassays. *PLoS One* 12, e0179636.
- (7) Gerhardt, K. P., Olson, E. J., Castillo-Hair, S. M., Hartsough, L. A., Landry, B. P., Ekness, F., Yokoo, R., Gomez, E. J., Ramakrishnan, P., Suh, J., Savage, D. F., and Tabor, J. J. (2016) An open-hardware platform for optogenetics and photobiology. *Sci. Rep. 6*, 35363.
- (8) Hannanta-Anan, P., and Chow, B. Y. (2016) Optogenetic Control of Calcium Oscillation Waveform Defines NFAT as an Integrator of Calcium Load. *Cell systems* 2, 283–288.
- (9) Richter, F., Scheib, U. S., Mehlhorn, J., Schubert, R., Wietek, J., Gernetzki, O., Hegemann, P., Mathes, T., and Moglich, A. (2015) Upgrading a microplate reader for photobiology and all-optical experiments. *Photochem. Photobiol. Sci.* 14, 270–279.
- (10) Basu, S., Gerchman, Y., Collins, C. H., Arnold, F. H., and Weiss, R. (2005) A synthetic multicellular system for programmed pattern formation. *Nature* 434, 1130–1134.
- (11) Gerchman, Y., and Weiss, R. (2004) Teaching bacteria a new language. Proc. Natl. Acad. Sci. U. S. A. 101, 2221–2222.
- (12) Farrell, C. M., Grossman, A. D., and Sauer, R. T. (2005) Cytoplasmic degradation of ssrA-tagged proteins. *Mol. Microbiol.* 57, 1750–1761.

(13) Purcell, O., Grierson, C. S., Bernardo, M. d., and Savery, N. J. (2012) Temperature dependence of ssrA-tag mediated protein degradation. *J. Biol. Eng.* 6, 10–10.

- (14) Zayner, J. P., and Sosnick, T. R. (2014) Factors That Control the Chemistry of the LOV Domain Photocycle. *PLoS One* 9, e87074.
- (15) Nash, A. I., McNulty, R., Shillito, M. E., Swartz, T. E., Bogomolni, R. a., Luecke, H., and Gardner, K. H. (2011) Structural basis of photosensitivity in a bacterial light-oxygen-voltage/helix-turnhelix (LOV-HTH) DNA-binding protein. *Proc. Natl. Acad. Sci. U. S. A. 108*, 9449–9454.
- (16) Christie, J. M., Gawthorne, J., Young, G., Fraser, N. J., and Roe, A. J. (2012) LOV to BLUF: flavoprotein contributions to the optogenetic toolkit. *Mol. Plant 5*, 533–544.
- (17) Pudasaini, A., El-Arab, K. K., and Zoltowski, B. D. (2015) LOV-based optogenetic devices: light-driven modules to impart photoregulated control of cellular signaling. *Front. Mol. Biosci.* 2, 18.
- (18) Motta-Mena, L. B., Reade, A., Mallory, M. J., Glantz, S., Weiner, O. D., Lynch, K. W., and Gardner, K. H. (2014) An optogenetic gene expression system with rapid activation and deactivation kinetics. *Nat. Chem. Biol.* 10, 196–202.
- (19) Reade, A., Motta-Mena, L. B., Gardner, K. H., Stainier, D. Y., Weiner, O. D., and Woo, S. (2017) TAEL: a zebrafish-optimized optogenetic gene expression system with fine spatial and temporal control. *Development 144*, 345–355.
- (20) Fluorescein, Certificate of Analysis, Standard Reference Material 1932 (2017) National Institute of Standards and Technology, Gaithersburg, MD.
- (21) Glantz, S. T., Berlew, E. E., Jaber, Z., Schuster, B. S., Gardner, K. H., and Chow, B. Y. (2018) Directly light-regulated binding of RGS-LOV photoreceptors to anionic membrane phospholipids. *Proc. Natl. Acad. Sci. U. S. A.* 115, E7720–E7727.
- (22) Inifinite Pro FI Bottom Sensitivity. Technical Note (2010) Tecan Group Ltd., Männedorf, Switzerland.